Victor Podsechin; Gerald Schernewski
Finite element modelling of flow and temperature regime in shallow lakes

In: Jan Brandts and Sergej Korotov and Michal Křížek and Jakub Šístek and Tomáš Vejchodský (eds.): Applications of Mathematics 2013, In honor of the 70th birthday of Karel Segeth, Proceedings. Prague, May 15-17, 2013. Institute of Mathematics AS CR, Prague, 2013. pp. 177–184.

Persistent URL: http://dml.cz/dmlcz/702944

Conference Applications of Mathematics 2013
in honor of the 70th birthday of Karel Segeth.
Jan Brandts, Sergey Korotov, Michal Křížek,
Jakub Šístek, and Tomáš Vejchodský (Eds.),
Institute of Mathematics AS CR, Prague 2013

FINITE ELEMENT MODELLING OF FLOW AND TEMPERATURE REGIME IN SHALLOW LAKES

Victor Podsechin[1], Gerald Schernewski[2]

[1] Department of Geophysics, University of Helsinki
P.O. Box 64, FI-00014 Helsinki, Finland
victor.podsechin@gmail.com
[2] Baltic Sea Research Institute Warnemünde (Institut für Ostseeforschung, IOW)
Seestraβe 15, D-18119 Warnemünde, Germany
gerald.schernewski@io-warnemuende.de

Abstract

A two-dimensional depth-averaged flow and temperature model was applied to study the circulation patterns in the Oder (Szczecin) Lagoon located on the border between Germany and Poland. The system of shallow water and temperature evolution equations is discretized with the modified Utnes scheme [4], which is characterized by a semi-decoupling algorithm. The continuity equation is rearranged to Helmholtz equation form. The upwinding Tabata method [3] is used to approximate convective terms. Averaged flow fields under prevailing wind conditions in August were calculated. The temperature variations were also simulated during the flood period in summer 1997. Simulation results are presented and limitations of the model are discussed.

1. Introduction

Wind induced flows in water bodies play an important role in dynamics of aquatic ecosystems. Water temperature, in turn, is one of the important physical parameter that affects limnological, biological processes. Especially in large shallow systems, like the lagoon, significant spatial differences in water temperature are possible. As a result biological and chemical processes may have different intensities in different regions of the lagoon. An accurate diagnosis and prediction of background physical processes, like currents and temperature variations is essential for correct understanding of aquatic ecosystems functioning. In shallow, well mixed water bodies a depth-averaged system of the so-called "shallow water" and temperature equations gives a rather good description of real systems.

2. Materials and methods

The dynamics of flow and temperature in shallow lakes can be described with vertically integrated equations of motion, continuity and heat transfer [1], given in vector form

$$\frac{\partial V}{\partial t} + (\nabla \cdot V)V + f \times V = -g\nabla\zeta + k\,|W|\,W - \frac{gn^2\,|V|\,V}{H^{4/3}} + \nu\Delta V, \tag{1}$$

$$\frac{\partial \zeta}{\partial t} + \nabla \cdot (HV) = 0, \tag{2}$$

$$\frac{\partial HT}{\partial t} + (\nabla \cdot V)HV = \mathrm{div}(\nu_T H \nabla T) + \frac{\alpha(T - T_a)}{\rho_0 C_p}. \tag{3}$$

In above, $V = (u, v)$ is a depth-averaged velocity vector, $H(x, y, t) = h(x, y) + \zeta(x, y, t)$ is the total water depth, ζ is the water surface elevation above a horizontal datum, h is the depth below datum, $W = (W_x, W_y)$ is the wind velocity vector, f is the Coriolis parameter, g is the acceleration due to gravity, n is the Manning roughness coefficient, k is the wind resistance coefficient, ν is the horizontal eddy viscosity, $\rho_0 = 10^3\,\mathrm{kg\,m^{-3}}$ is water density, $C_p = 4.18710^{-3}\,\mathrm{J\,kg^{-1}\ ^\circ C^{-1}}$ is a specific heat capacity of water, T is water temperature (°C), T_a is air temperature (°C), α is the bulk heat exchange coefficient ($\mathrm{W\ m^{-2}\ ^\circ C^{-1}}$). It is estimated using an empirical dependence on wind speed W, ($\mathrm{ms^{-1}}$), see [1]:

$$\alpha = 5.7 + 3.8W. \tag{4}$$

The boundary conditions of system (1)–(2) are as follows (cf. [1]):

$$\text{land boundary:} \quad V|_{B_1} = 0, \tag{5}$$

$$\text{liquid boundary:} \quad \zeta|_{B_2} = \zeta|_B(t). \tag{6}$$

When $\nu = 0$ the governing equations (1)–(2) constitute a system of quasi-linear hyperbolic partial differential equations. In this case the non-slip boundary condition (5) is replaced with the slip one

$$V \cdot n|_{B_1} = 0, \tag{7}$$

where n is the unit vector normal to the boundary of the solution domain. Zero initial conditions

$$V = \zeta|_{t=0} = 0 \tag{8}$$

are frequently used in practical applications to start the time integration.

For temperature equation (3) the no-flux boundary condition was applied along the solid boundary. The observations of time-varying inflowing water temperature in the river Oder altogether with estimated values of inflowing mean cross-section

velocity (T. Neumann, pers. com.) and time-series of wind in the Pomeranian Bight were used to drive the combined flow and temperature model.

Using a time-splitting algorithm [4] the momentum equation (1) is discretized as follows:

$$\frac{V^* - V^m}{\tau} + (\nabla \cdot V^m)V^* + f \times V^m = k \left|W^{m+1}\right| W^{m+1} - \frac{gn^2 \left|V^m\right| V^*}{H^{4/3}} + \nu \triangle V^*, \quad (9)$$

$$\frac{V^{m+1} - V^*}{\tau} = -g\nabla\zeta^{m+1}. \quad (10)$$

When the time derivative is approximated with the forward difference the continuity equation takes the form:

$$\zeta^{m+1} = \zeta^m - \tau\nabla \cdot HV^{m+1}. \quad (11)$$

Multiplying equation (10) by H, taking the divergence and substituting it in place of $\nabla \cdot HV^{m+1}$ into (11), the Helmholtz approximation of the semi-implicit continuity equation is obtained

$$[1 - \tau^2 g\nabla \cdot H\nabla]\zeta^{m+1} = \zeta^m - \tau\nabla \cdot HV^*. \quad (12)$$

The calculations are organized in the following way: an intermediate velocity V^* is calculated by (9), the water level elevation ζ^{m+1} is predicted by (12) and the corrected velocity V^{m+1} is obtained from (10).

The space domain Ω is divided into a sum of linear triangular elements. Unknown variables are approximated as series of basis functions

$$V \approx \sum_{j=1}^{N} V_j \cdot \varphi_j, \quad \zeta \approx \sum_{j=1}^{N} \zeta_j \cdot \varphi_j, \quad T \approx \sum_{j=1}^{N} T_j \cdot \varphi_j, \quad (13)$$

where N is the number of mesh nodes and φ_j are the global basis functions. After substituting the decompositions (13) to (3), (9), (10), and (12), multiplying according to the Galerkin method by the weight-functions φ_i^T, integrating over Ω and applying the Gauss theorem for the second-order terms, the system of linear algebraic equations is derived

$$(M + \tau(CONV + D + gn^2F))V^* = M(V^m - \tau(f \times V^m - k \left|W^{m+1}\right| W^{m+1})) + \tau \int_B \varphi_i \nu \frac{\partial V}{\partial n} dB, \quad (14)$$

$$(M + g\tau^2 K)\zeta^{m+1} = M\zeta^m - \tau G(HV)^* + g\tau^2 \int_B \varphi_i H \frac{\partial \zeta}{\partial n} dB, \quad (15)$$

$$MV^{m+1} = MV^m - \tau g G\zeta^{m+1}, \quad (16)$$

$$(M + \tau(CONV + D^*))HT^{m+1} = MHT^m + \tau\frac{\alpha}{\rho C_p} M(T - T_a)^m, \quad (17)$$

where the global matrices are compiled as follows:

$$M = \int_\Omega \varphi_i \cdot \varphi_j^T d\Omega, \quad D = \int_\Omega \nu \nabla\varphi \cdot \varphi_j^T d\Omega, \quad D^* = \int_\Omega \nu_T \nabla\varphi_i \cdot \nabla\varphi_j^T d\Omega, \tag{18}$$

$$F = \int_\Omega \varphi_i \cdot \varphi_j^T \cdot \frac{|V^m|}{H^{4/3}} d\Omega, \quad G = \int_\Omega \nabla\varphi_i \cdot \varphi_j^T d\Omega, \quad K = \int_\Omega \nabla\varphi_i \cdot H \nabla\varphi_j^T d\Omega. \tag{19}$$

The CONV denotes the global convective matrix, modified according to the upwinding Tabata scheme [3]. The systems of linear equations (14)–(17) are solved sequentially using a direct Gaussian elimination method [1].

3. Numerical results

In the first step a linear triangular mesh of 2240 nodes and 3845 elements covering the Oder lagoon was generated (Fig. 1) and linked to depth information. This grid density with a slightly simplified bathymetry was chosen to keep the computation time reasonable. During the Oder flood in summer 1997, the total simulation period of 20 days with simulation time steps of 5 minutes was used for flow field calculations. The Manning roughness coefficient of $0.015\,\mathrm{m}^{-1/3}\mathrm{s}$, the horizontal diffusion coefficient equal to $0.01\,\mathrm{m}^2\mathrm{s}^{-1}$, and the Coriolis parameter of $1.174 \cdot 10^{-4}\,\mathrm{s}^{-1}$ were applied.

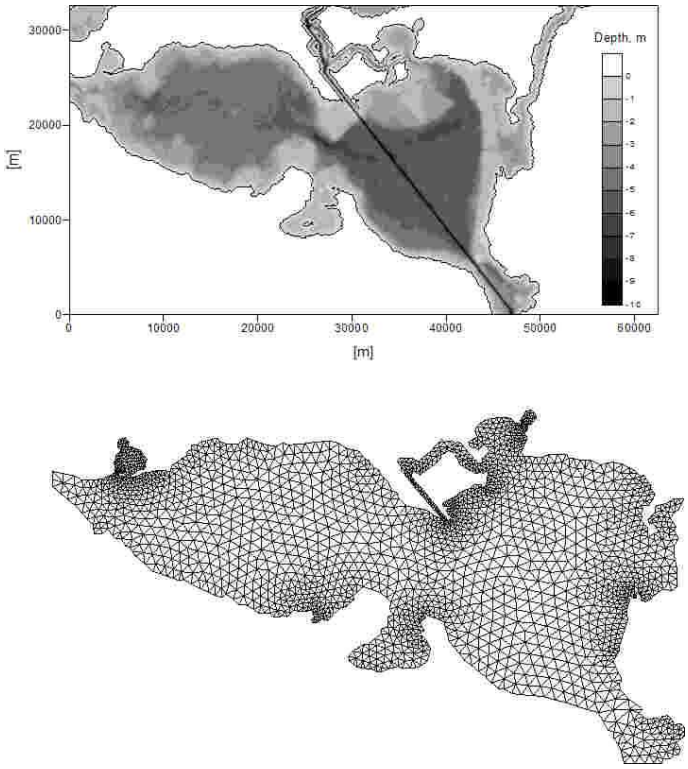

Figure 1: Bathymetric map and triangular mesh of the Oder Lagoon.

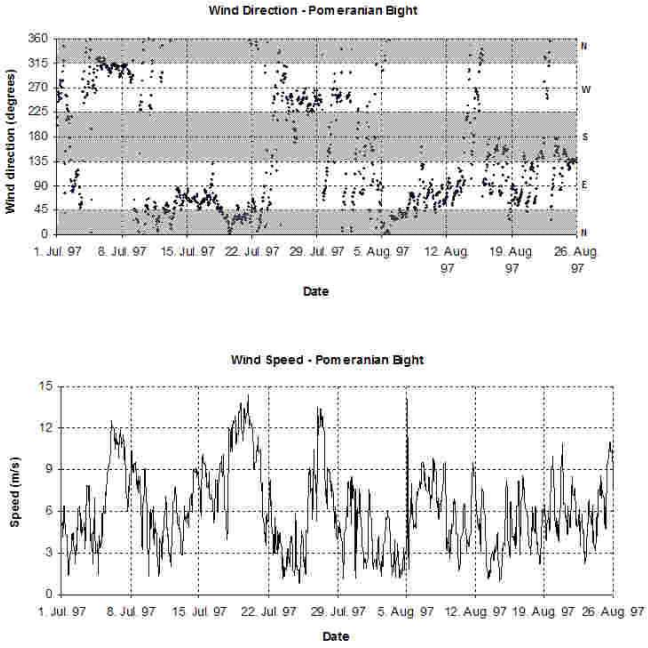

Figure 2: Wind direction and wind speed in the Pomeranian Bight during the Oder flood in July and August 1997.

In steady-state simulations a constant and spatial uniform wind field as well as constant water discharge was used. Wind data was available from an automatic recording station in the Oder Bight (Fig. 2) and for several periods from the centre of the lagoon, too. Wind speed from Oder Bight was adapted to the situation in the lagoon by multiplication with the empirical derived factor of 0.46 (Spiegel pers. com). According to Mohrholz and Lass [2] the discharge from the lagoon into the Baltic Sea varied depending on the prevailing wind direction (13–19 % Peene Strait, 8–14 % Dziwina Strait, 73 % Swina Strait) but was kept constant with time. Intrusion of seawater was neglected.

Depending on the general atmospheric situation wind from east and west is dominating during late summer. The flow field for these two typical wind situations were simulated assuming a river discharge into the lagoon of about $300\,\mathrm{m^3 s^{-1}}$ (Fig. 3). Under common late summer discharge situations the flow field is to a significant amount determined by wind conditions. In general, the simulated flow velocities are low and water masses need about 50 days to pass the lagoon and to enter the western bay (Kleines Haff). The flow in the deep channel, crossing the lagoon, shows some special behaviour, with reduced flow velocities. The water transport through the eastern and western shallower regions is significant faster. In the central parts of the Kleines Haff the flow velocities are low. But close to both shores a coastal jet with increased flow and transport speed occurs. Under these conditions the shores are to a higher degree affected by Oder water than other areas of the bay.

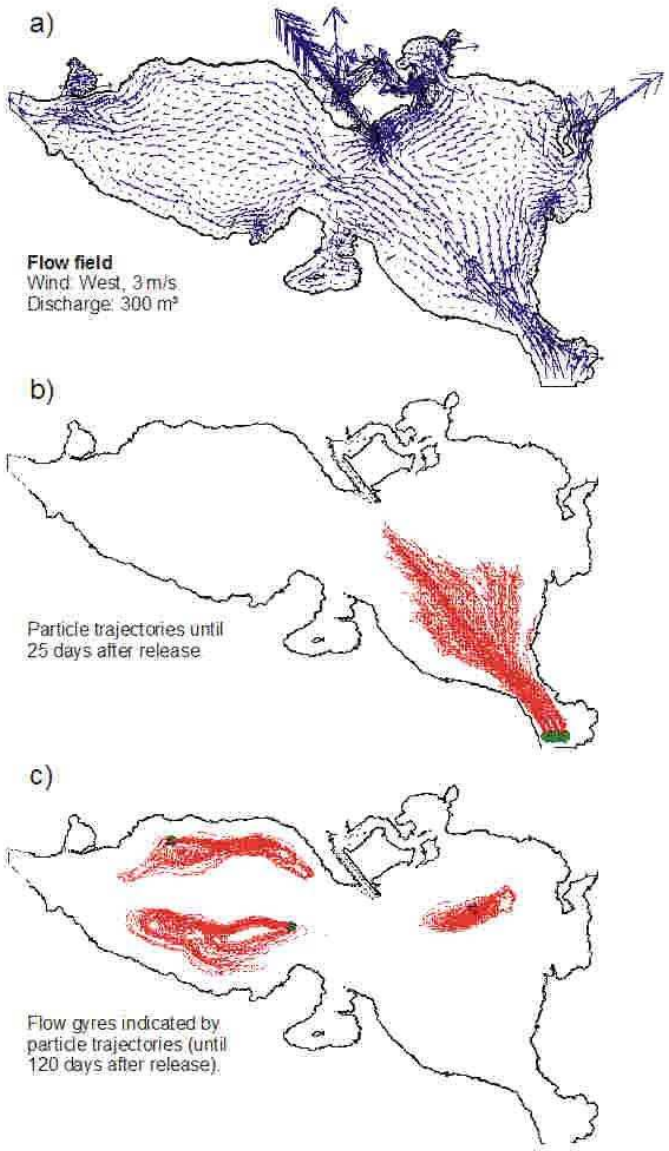

Figure 3: Average two-dimensional flow field under typical August weather conditions. An average Oder discharge into the lagoon of $300\,\mathrm{m^3 s^{-1}}$ and a mean wind of $3\,\mathrm{ms^{-1}}$ from west was applied. The trajectories of passive particles moving with currents are shown 25 and 120 days after release in different locations.

Despite these coastal jets water needs 70 days to pass this bay and 120 days to pass the whole lagoon from river mouth to the Peene strait. This slow transport and water exchange allow independent local ecological dynamic, like algal bloom in the bay. Under similar water discharge but west wind conditions a quite different flow pattern prevails (Fig. 3). The simulations show a relatively fast transport of 26 days across the lagoon via the deep channel. All shallower parts on the right- and left-hand

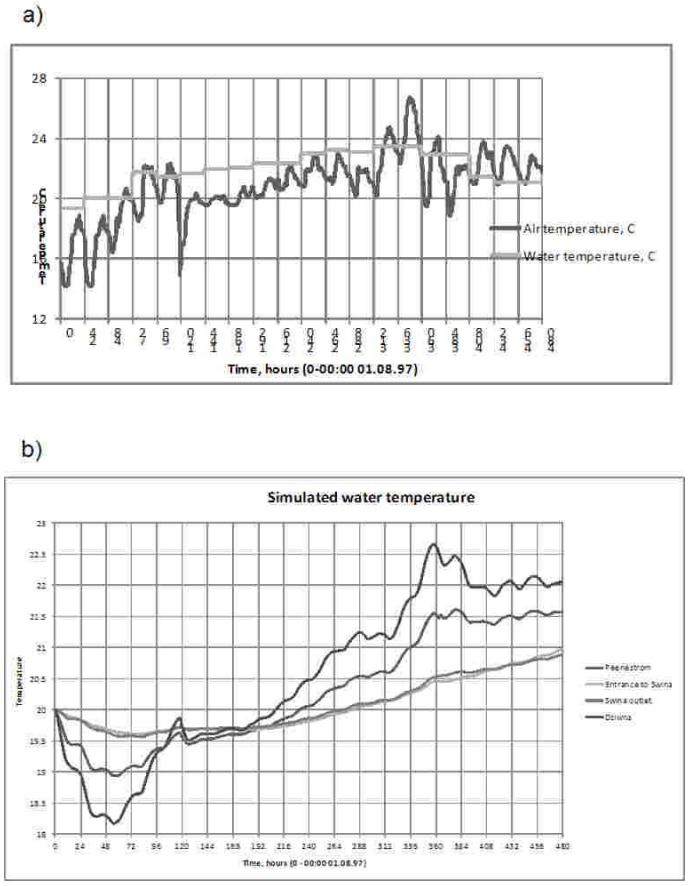

Figure 4: The Oder Lagoon between August 1 and August 20, 1997. a) Measured air temperature and simulated water temperature, b) Simulated water temperatures in different areas of the lagoon.

side show much lower current speeds. In several areas in the Kleines Haff as well as in the eastern part pronounced large eddies occur and limit the water exchange (Fig. 3c). Interpreting the figures, one has to keep in mind that the simulations yield depth-averaged flow velocities, that constant wind and discharge were applied and seawater intrusions were disregarded. These simplifications limit general statements.

Results of dynamic simulation under the time varying meteorological conditions show that the temperature regime of the Oder lagoon is strongly influenced by air temperature fluctuations. The dependence of the bulk heat transfer coefficient on wind speed (4) additionally accelerates the response of depth-averaged water temperature to changes in atmospheric conditions. This is clearly reflected in Fig. 4b showing simulated time-series of water temperature in different parts of the lagoon. Shallow near coastal areas exhibit higher and faster changes than deeper parts located in the vicinity of the navigational channel. During night the spatial temperature differences in the lagoon are significant lower than during day. In August 1997,

for example the spatial temperature difference exceeded 2°C during the day and was below 1°C in the night. Due to the flood, the flow velocity in the lagoon was much higher compared to other years and spatial water exchange increased. Under common summer conditions we can expect significant higher spatial temperature differences.

Acknowledgements

This work was supported by the DFG (Deutsche Forschungsgemeinschaft), Academy of Finland (von Humboldt Fund), Finnish Ministry of Environment, and Grant MTM2011–24766 of the MICINN (Spain).

References

[1] Benque, J.-P., Haugel, A., and Viollet, P.-L.: *Engineering applications of computational hydraulics*. Vol. II, Pitman Advanced Publishing Program, 1982.

[2] Mohrholz, V. and Lass U.: Transports between Oderhaff and Pomeranian Bight a simple barotrophic box model. Dt. Hydrogr. Z. **50** (1998), 371–383.

[3] Tabata, M.: A finite element approximation corresponding to the upwinding finite differencing. Mem. Numer. Math. **4** (1977), 46–63.

[4] Utnes, T.: A finite element solution of the shallow-water wave equations. Appl. Math. Model. **14** (1990), 20–29.